Volume Title
ASP Conference Series, Vol. **Volume Number**
Author

A Path to NIST Calibrated Stars over the Dome of the Sky

Peter Zimmer[1], John T. McGraw[1], Daniel C. Zirzow[1], Claire Cramer[2], Keith Lykke[2] and John T. Woodward IV[2]

[1]*University of New Mexico, MSC 07-4220, 1 Univ. of New Mexico, Albuquerque, NM 87131*

[2]*National Institute of Standards and Technology, 100 Bureau Drive, Stop 1070, Gaithersburg, MD 20899*

Abstract. The UNM Measurement Astrophysics group is currently constructing and testing a mobile instrument suite that includes a multi-wavelength backscatter lidar, stellar spectroradiometer and cameras (visible and thermal infrared) that will provide real-time atmospheric transmission metadata in the column of atmosphere through which a supported telescope is observing. The design, operation and calibration of the lidar (the Facility Lidar for Astronomical Measurement of Extinction - FLAME) and spectroradiometer (the Astronomical Extinction SpectroPhotometer - AESoP) are detailed.

The first task of this instrument suite will be to help create a new set of standard stars radiometrically calibrated to NIST standards. Initially this will be done for bright stars across the wavelength range 350nm to 1050nm at 1nm spectral resolution with measurement accuracy better than 1% per spectral resolution element by calibration to NIST silicon detectors.

Because these standard stars will support both ground- and space-based observations, our proposed evolution of calibration begins with suitable bright optical standards and then adds measurements into the infrared. Following optical/infrared calibration of bright stars we plan to calibrate fainter stars, ultimately to V∼18, both in the optical and near infrared.

1. NIST Stars

The Measurement Astrophysics Research Group at the University of New Mexico and the National Institute for Standards and Technology (NIST) have been collaborating on techniques and instrumentation designed to produce a new generation of absolutely calibrated standard stars directly traceable to NIST laboratory radiometric standards. Previous efforts, most notably those of Oke & Schild (1970), Hayes et al. (1975), and Tüg et al. (1977) but see also Megessier (1995) and references therein, used emissive sources, either lamps or molten metal blackbodies, placed some long distance from the telescope as the calibration standard and alternated observing the standard star and the source. Over the last decade, NIST has moved away from emissive standards in the visible and near-infrared and now uses detector based standards, such as silicon and InGaAs photodiodes (Larason et al. 1996; Yoon et al. 2003), that have been calibrated against primary optical standards (Brown et al. 2006; Smith et al. 2009). In addition to calibration source systematics, variable atmospheric transmission contributed the other

major limiting factor to these previous calibration efforts, both the transmission between star and telescope and between the telescope and calibration source (Hayes & Latham 1975).

The goal of NIST Stars is to produce a new set of standard stars calibrated to NIST detector-based radiometric standards. The current effort is aimed at producing ~100 stars brighter that $m_V = 6$ over the entire sky, calibrated from 400 nm to 1000 nm to better than 1% accuracy in 1 nm bins. Using detectors as reference standards instead of emitters means that atmospheric attenuation between the source and telescope can be made very small by illuminating the standard detector and telescope under calibration through nearly identical atmospheric paths. Additionally, a number of other advancements in the intervening decades allow for better determination of the extinction between the telescope and the top of the atmosphere, in particular more advanced atmospheric models (e.g. MODTRAN 5 (Berk et al. 2005)) and new ways to directly probe the atmosphere, such as lidar (Zimmer et al. 2010).

1.1. Applications

The primary driver for this calibration effort is to benefit observational astronomy by allowing a path to calibrate measurements, both within a given data set and between observations made with radically different instruments under a range of local observing conditions, to a common unit system available to all ($W/m^2/nm$). This includes measurements made both with ground-based and with space-based observatories. In addition to astronomical applications, there are numerous other optical systems, both terrestrial and otherwise, in use worldwide carrying out missions for weather and climate remote sensing, geospatial intelligence, and defense. All of these various sensors can be made more accurate if appropriate radiometric standards are available. Moreover, once a set of absolute standards have been created, relatively simple instrumentation can be used to measure atmospheric transmission (see Section 5.2).

1.2. Initial targets

Our initial calibration efforts have been targeted at stars that already have a calibration pedigree. Vega will be calibrated, not because it is a particularly good choice of standard star (has a debris disk (Mountain et al. 1985), rapid, pole-on rotation (Peterson et al. 2006), possibly variable (Engelke et al. 2010)), but because of the history of its use as a standard, thus allowing ties back to the extensive history of astronomical photometry (see Landolt in these proceedings). 109 Viginis is another target that has been frequently used as a calibration standard (Tüg et al. 1977) and Sirius. The initial target list is rounded out by 19 stars from the Next Generation Spectral Library (Heap & Lindler 2007), chosen for appropriate brightness, declinations observable from northern hemisphere observatories, lack of nearby confusion sources and not flagged as variable in the HIPPARCOS database (van Leeuwen et al. 1997). Vega (Bohlin & Gilliland 2004) and the NGSL targets all have spectra obtained by STIS on HST, which is calibrated (relative) against model white dwarf atmospheres (Bohlin 2000). Using targets with measured top-of-the-atmosphere spectral energy distributions (SED) will initially help in the development of our calibration process. Differences between our measurements and STIS measurements, both within a given star's SED and the relative measurements between stars, must be understandable and resolved. NIST Stars then can provide a consistent and quantified absolute flux scale to the ensemble of stars and together establish the HST white dwarf sample as secondary absolute standards.

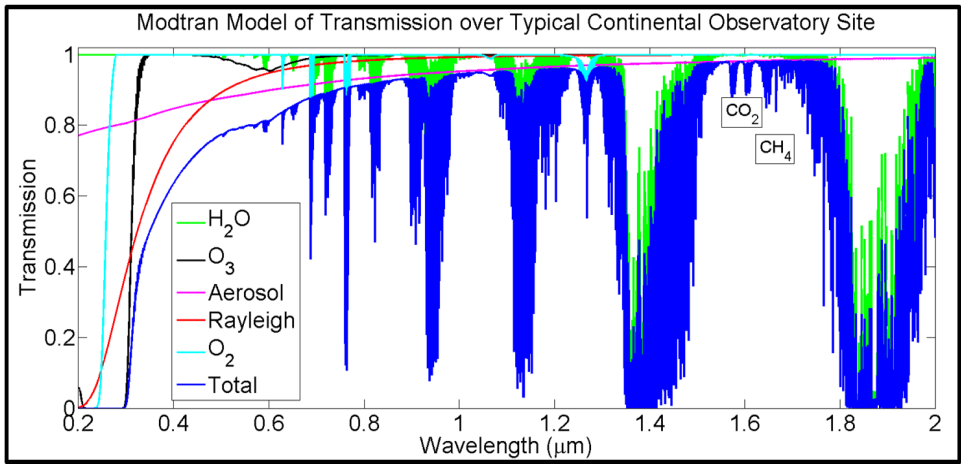

Figure 1. The blue line plots total atmospheric transmission as a function of wavelength in the near-UV thru short wave IR spectral regions as modeled by MODTRAN using nominal atmospheric conditions for Albuquerque, NM. The other lines break down the transmission into its various component contributions.

2. Measurement Approach

Because variable atmospheric transmission constitutes the source of the largest known systematic errors for calibrating standard stars, that is where we focus our efforts. The usual approach of measuring atmospheric extinction using a Langley extrapolation technique, where stars are measured at a range of airmass and the total extinction is extrapolated to zero airmass, assumes that the atmosphere is homogeneous at a given altitude (either plane parallel or spherically symmetric about the center of the Earth) and that the changes, spatial and temporal, in atmospheric transmission over time are small compared to the desired photometric accuracy. A better approach is to measure the transmission of the column of air through which calibrations are being made.

2.1. Two Instrumental Techniques for Two Categories of Extinction

Figure 1 shows an atmospheric transmission spectrum generated in MODTRAN for a typical desert observing site conditions. The constituents of that spectrum can be broken into two broad categories based on spectral signature: those that varying rapidly with wavelength such as molecular absorption from H_2O and O_2 and those that vary slowly (or not at all) with wavelength, such as clouds and aerosols. We match this breakdown with two instruments: a calibrated spectrophotometer that can very precisely measure the relative spectrum of atmospheric transmission as imprinted on a stellar spectrum and a calibrated multiwavelength backscatter lidar, which can measure the total atmospheric transmission at a few specific laser wavelengths.

2.2. Calibrated Spectrophotometry

By calibrated spectrophotometry we mean observing the candidate standard star with a low resolution ($R \sim 1000$) spectrometer that has been irradiance calibrated such that the absolute throughput of the instrument and associated uncertainties are known. The resulting stellar data is the product of the stellar SED and spectrum of atmospheric

transmission. In the case of candidate standards with HST spectra, the relative stellar SED is known and thus all that remains is to determine a wavelength independent (i.e. gray) scale factor. For targets where the SED is not measured above the atmosphere, models of the particular target's atmosphere can be used to break apart the effects of atmospheric transmission from features of the star. Fortunately, while the radiative transfer physics of stellar atmospheres and Earth's atmosphere is the same, under most circumstances, the constituents of each are quite different and thus separable.

2.3. Calibrated Lidar

In our approach, the calibrated lidar system transmits pulsed laser light at multiple wavelengths and detects the elastic backscatter signal of the constituents of Earth's atmosphere. A telescope aligned with the transmitted laser light collects the scattered photons and detected light is time-gated such that the range from which a particular photon returned is known to high accuracy. The signal from an elastic lidar is well modeled by the so-called lidar equation (Eqn. 1) (Kovalev & Eichinger 2004):

$$N(r) = N_0 \eta \frac{A}{r^2} \left(\frac{3}{8\pi} \beta_m(r) + \frac{P(r)}{4\pi} \beta_a(r) \right) e^{-2\tau(r)} \tag{1}$$

where $N(r)$ is the number of photons returned from a given range, r, N_0 is the number of photons launched from the transmitter, A is the telescope collecting area, η is the system throughput, β_m & β_a are the volume scattering coefficients for molecules and aerosols respectively (where the $\frac{3}{8\pi}$ is the Rayleigh backscatter phase function), P(r) is the backscatter phase function for aerosols and $\tau(r)$ is the extinction along the laser path from the ground to a the range r. The factor of two in the exponent appears because the light must propagate both up and back to the given range, thus sees the path attenuation twice.

With our measurement approach, in order to measure the transmission of the atmosphere (the exponential term in Eqn 1) we need to achieve two things: first we must calibrate the terms on the left hand part of Eqn 1, N_0, η, and A. Calibrating N_0 is simply a measurement of the transmitted laser power, which is not all that challenging except that the transmitted laser beam can be large (200mm and larger) and the power can be large (Watts), but otherwise simply requires a precise and accurate power meter. Calibrating the other two terms is identical to calibrating the irradiance response of the spectrophotometer, save that it only needs to be done at the laser wavelengths.

The second requirement is that we find a portion of the atmosphere where we know what β_m and β_a are based on other measurements and that said portion of the atmosphere is sufficiently high in altitude so that the bulk of the total transmission is coming from constituents below it. In our case, we choose to use the middle stratosphere, 30-40km above sea level, because it is high enough to be above the bulk atmospheric attenuation, low enough to be below altitudes where gravity waves modulate the density with amplitudes above 0.1%, and is constituted by mostly well-mixed air that is stable and routinely measured by radiosondes. Thus we are high enough that the aerosol backscatter is negligible (though we will test this) and β_m is measured and doesn't change much, so the transmission can be accurately measured from the strength of the Rayleigh return from the stratosphere.

3. The Astronomical Extinction Spectrophotometer (AESoP)

AESoP has been designed to be a small, affordable, replicable instrument for making calibrated spectrophotometric measurements of bright stars to accurately measure atmospheric transmission. Integral to the AESoP concept is that the entire system, including the calibration hardware, should be easily portable. This allows AESoP to be moved to various observing sites where it can support observations being taken with other, larger science telescopes and also move between observatory sites to maximize seasonal patterns, such as observing from California during the southwest monsoon that shuts down observatories in Arizona, New Mexico and Texas.

3.1. The Spectrometer

AESoP is an objective grating spectrometer built around a 106mm Takahashi FSQ-106ED apochromatic refractor and a Newport Richardson 90 lines/mm transmission grating blazed at 700nm. This combination was chosen to offer a good dispersion and free spectral range match to typical off-the-shelf CCDs. We chose a design with a filled circular pupil to simplify the collecting area measurement required for irradiance calibration. Because we were targeting bright stars to begin with, we needed to compromise between collecting area, scintillation and cost, where a roughly 100mm aperture fit these requirements. The aperture is stopped down slightly from 106mm to roughly 100mm with a precision machined invar aperture plate, which ensures the collecting area is not changing more than 100 ppm over the wide temperature ranges encountered at observatory sites. The aperture plate has been optically scanned and measured to have a collecting area of $7827.17 \pm 0.01 mm^2$.

The optical layout of AESoP is designed to be as simple as possible. After the aperture plate and grating, the refracting telescope is tilted slightly ($\sim 4^\circ$ to the grating normal) so that the middle of the first order spectrum at 780nm is parallel to the optical axis of the telescope. At the output of the refractor is a photometric shutter, focuser and filter wheel with order blocking filters. The CCD camera is a FLI Proline with an E2V 4210 chip (back-illuminated 2048 x 512 15μ pixels). The first order spectrum covers 525nm - 1040nm with 0.28nm pixel resolution and the second order spectrum cover 360nm-555nm with 0.14nm pixels. Because there is no slit, the spectral resolution is fundamentally limited by the PSF, though the image scale was chosen to undersample typical seeing conditions thus minimizing the effects of seeing variations on the delivered spectral resolution.

3.2. Calibration Transfer Telescope

The way AESoP is calibrated is by using a second telescope as a transfer standard. Because observatory environments are dirty, any telescope exposed to the sky accumulates dust (and worse) over time which changes its irradiance response. Because of this, AESoP needs to be calibrated repeatedly over the course of a night. Thus there is a need for a calibration standard that is not exposed to the sky but can accurately placed at the same distance from a calibration source as AESoP and cover a similar source brightness dynamic range.

Our solution to this problem is the CAL telescope, an optical system designed to be very similar to AESoP, but with no dispersive element. CAL is an identical Takahashi refractor with a nearly identical precision invar aperture plate that mounts below AESoP so that the apertures are coplanar. For a detector CAL uses a small achromatic lens to

Figure 2. The picture to the left shows AESoP and CAL in the newly delivered mobile observatory with the roof open and the instruments fully elevated. The image on the right shows AESoP and CAL in their lowered calibration position looking down their baffles.

create a pupil image on a CCD. The CCD is read out in TDI mode and binned, by an amount depending on the intensity of the calibration signal, into a one dimensional time resolved measurement of the intensity of the pupil image. The proof-of-concept detector for CAL had a measured noise equivalent power (NEP) of $92aW/\sqrt{Hz}$ and a new sensor optimized for this operational mode is expected to be delivered soon and should improve this figure of merit by a factor of 5 or more. This is in contrast to the photodiode that was originally in place as the calibration detector which had a NEP of $> 600aW/\sqrt{Hz}$.

CAL is designed to be easily removable from the telescope mount so that it can be sent to NIST and calibrated, one wavelength at a time, against NIST standard photodiodes in the Telescope Calibration Facility (TCF - Smith et al. (2009)). When attached to AESoP, both systems view the local calibration source, which is a monochromator with a halogen bulb that feeds a small multimode fiber. The fiber output is at the focal point of a 16" f/4 parabolic collimator mirror. The collimated beam overfills both AESoP's and CAL's apertures, and because they are the same distance from the collimator, small errors in the output beam divergence don't create irradiance differences. The monochromator is stepped through wavelength and the calibration of CAL can be transferred to AESoP. When not in operations, CAL is covered to minimize environmental contamination.

3.3. Mobile Observatory Layout

AESoP and all of the calibration apparatus are contained in an 8'x16' trailer that allows the entire system to be moved between observation sites with minimal setup time (see Figures 2 & 3). The trailer floorplan is split into two 8' square sections, one with AESoP and CAL and the other with the calibration source hardware. A small window between the two chambers is opened during calibration, allowing AESoP and CAL to view the collimator mirror and otherwise closed to keep out dust. The telescope side has a retracting roof to allow access to the sky.

AESoP and CAL are co-mounted on a Software Bisque Paramount ME, along with an autoguider and other auxiliary equipment. The Paramount is attached to a vibration-

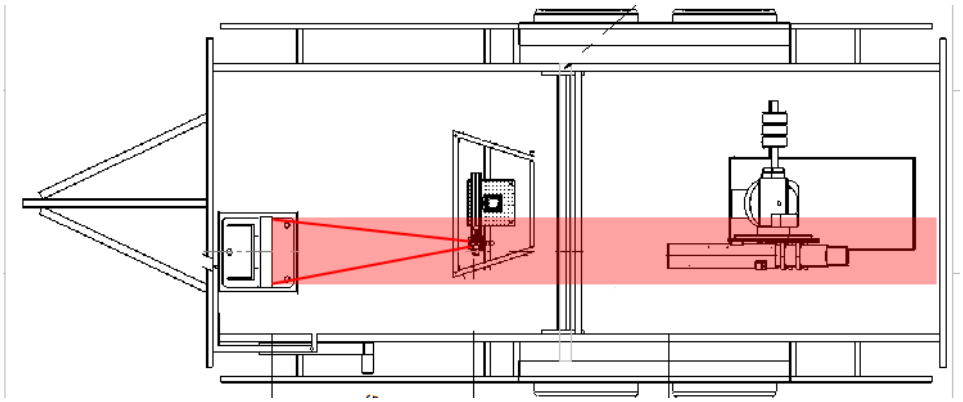

Figure 3. This drawing shows the mobile observatory floor plan with the system in its calibration position. Calibration light is projected out of a fiber just to the left of the middle partition into the 16 inch collimator mirror at the left. The collimated beam illuminates both AESoP and CAL, one wavelength at a time, allowing transfer of the CAL irradiance calibration onto AESoP.

isolated elevating platform to allow AESoP to be raised up and peer over the side of the trailer at terrestrial sources on the horizon as a calibration cross-check and also change how AESoP and CAL are illuminated by the calibration system to test for systematic errors in illumination during the calibration transfer process.

3.4. Construction Status

The last missing large component, the trailer, arrived the week prior to this conference. Integration and testing have begun with anticipated first light in early June 2012 and automated science operation by the end of summer.

4. Facility Lidar for Astronomical Measurement of Extinction (FLAME)

Elastic backscatter lidars such as FLAME are relatively simple optical systems consisting of a pulsed laser, beam expansion optics, a receiver telescope and a detector that can time the return of the photons scattered by the atmosphere. There are many other sorts of lidar that can reveal the atmosphere in great detail, but they are more complicated and thus more expensive, instruments, and most do not have the throughput to retrieve the transmission from the stratosphere with high precision on minute timescales. FLAME will produce a wealth of other information about the atmosphere through which it transmits, but was designed to measure Rayleigh scattering from the middle stratosphere. Based on our previous experience with ALE (Zimmer et al. 2010), the enhanced capability of FLAME should readily achieve this goal.

4.1. Laser and Transmitters

The basis for FLAME is an Ekspla NT-220 three harmonic Nd:YAG system that outputs 3W at 1064nm, 2W at 532nm and 1.5W at 355nm, all with ~6ns pulse widths at 1500Hz, which leaves enough time for a given pulse to travel 100km and back before the next pulse launches. The 1064 and 532 channels are fed directly into individual

Figure 4. An image of FLAME from an assembly test is shown with one transmitter (the white 200mm telescope in the upper left) and one 75mm short range receiver (small black tube on top) attached.

400 micron mulitmode fibers, while the 355nm channel is first sent through a ring cavity pulse stretcher (Kojima & Nguyen 2002) to reduce the peak pulse power below the fiber damage threshold and then fed into a 400 micron fiber. The fibers route the laser light to the transmitter optics mounted and co-aligned on the main receiver telescope. The light from each fiber is collimated to 20mm diameter and ~1% is split to a power meter, the remainder continues and the 532 and 355 channels are combined with a harmonic separator dichroic mirror. Two 200mm diameter commercial Newtonian telescopes, one for 355/532 and one for 1064 provide the final beam expansion.

4.2. Receiver Optics

FLAME's has three 75mm short range receivers, one for each laser wavelength, which are mounted and co-aligned with the main receiver telescope. Each one consists of an objective lens, field stop, collimating lens, 2nm wide narrowband filter and Fabry lens which make a pupil image at the detector, where all the glass and coatings are optimized for the particular wavelength. The 75mm aperture was chosen to optimally cover the dynamic range of signals from 100m to 10km altitude where the long range receiver will saturate. FLAME's main receiver is based around a custom Planewave 20" RC telescope (see Figure 4) on a Mathis Instruments alt-az mount that collects the return from all three laser wavelengths. There is a common field stop placed at the 10 km conjugate focal point which aids in the rejection of out-of-focus light from lower altitudes. The incoming light is then collimated by a triplet achromat that provides a 15mm diameter beam which is split by dichroics into individual 1064, 532 and 355nm channels. Each of those channels then passes through a 2nm bandpass filter, a Fabry lens and a secondary field stop before making a pupil image at the detector.

4.3. Detector System

The detectors for the 355nm and 532nm channels are Licel packaged Hamamatsu photomultiplier tubes (R9880U-210 and -20 respectively). The output of each is input to a Fast-COMTEC discriminator amplifier that provides two outputs, one shaped NIM output for pulse counting and one unshaped for analog detection. Pulse counting is provided by Fast-COMTEC P7882 PCI cards and analog detection is provided by a GaGe 8-channel 25MHz digitizer with on board signal averaging. The detector for the 1064nm channel is still under consideration. The resulting analog and photon counting profiles are accumulated in software into one minute profiles, except for the analog return below 10km, which is kept at the raw 0.6s temporal resolution, primarily to make pretty pictures.

4.4. Mobile Observatory Layout

FLAME will be housed in a mobile observatory trailer similar to AESoP's that is currently under construction with an expected delivery date of June 2012. The main receiver will be house on the side with the sliding roof and on a vibration isolated extensible platform so that is can point over the trailer walls. The other half of the trailer will contain the laser and calibration power meters.

4.5. Calibration System

As indicated in Section 2, in order to accurately measure atmospheric transmission both the transmitted power and irradiance sensitivity of FLAME need to be measured. The transmitted power is continually monitored by the power meter at the output of the fiber that feeds the transmitter. However, the throughput of the subsequent optics will change with time, thus the total output power needs to be periodically calibrated using a power meter that can accept a 200mm, 3W input beam. Two of these systems, one for each transmitter, would be at opposite side of the trailer where FLAME can point at them with the roof closed and are currently being designed. These systems would be calibrated in the NIST TCF in the same way as CAL.

The irradiance calibration of the receivers is undertaken in a manner similar to AESoP. A calibration transfer telescope similar to CAL, save for a filter wheel to select narrowband filters identical the the ones in the receivers, and calibrated at NIST in the same way as CAL, is mounted and co-aligned with FLAME. Both twilight sky to provide a diffuse source and bright stars to provide point sources would be observed by the FLAME receivers and FLAME's calibration telescope which would cycle between filters.

4.6. Current Status

Except for the mobile observatory trailer, all of the major components of FLAME have been acquired and are awaiting delivery of the trailer for integration and testing.

5. Using FLAME and AESoP to Create NIST Stars

Having acquired calibrated bottom-of-atmosphere spectra of bright stars with AESoP and calibrated monochromatic transmissions from FLAME, we must intelligently combine these data to extract the top-of-the-atmosphere calibrated spectral energy distribution of the observed stars.

5.1. Making Standard Stars

In order to produce the calibrated bottom-of-atmosphere spectrum, the measured spectra from AESoP must have the irradiance calibration derived from the wavelength-by-wavelength transfer from CAL to AESoP. This provides the tie between measured photoelectrons and $W/m^2/\mu m$. Next we ratio this calibrated spectrum to the best known (measured or modeled) top-of-atmosphere spectrum of the source star. The ratio represents the combination of atmospheric transmission and any calibration or other unresolved systematic errors.

The measured FLAME lidar returns will yield the absolute transmission at each laser wavelength, pinning the absolute energy scale at those wavelengths. Other auxiliary measurements of atmospheric parameters, especially surface pressure, radiosonde vertical profiles of temperature and humidity, local GPS precipitable water vapor measurements (Bevis et al. 1994), satellite measurements of ozone column depth, etc. are also compiled to inform the process of fitting the atmospheric transmission profile. Aside from the relationship between surface pressure and total Rayleigh scattering and oxygen absorption, these other measured quantities are not sufficiently accurate to use directly, but rather provide a starting point and a range of acceptable atmospheric parameters.

The fitting process at present uses a grid of MODTRAN 5 models created across the range of expected atmospheric parameters and airmass in a lookup table. The grid quadrature was chosen so that intermediate changes are well-represented by linear interpolation between points at the 0.1% or better level. The spectral resolution element is estimated using the cross-dispersion profile of the spectrum. Recovery of stellar lines in the middle of strong atmospheric absorption bands is likely to be problematic, but we are working with the authors of MODTRAN on techniques to improve this.

5.2. Using Standard Stars

Once absolute calibration has been established for a set of stars, AESoP or other similar calibrated spectrophotometers can be used to derive the atmospheric transmission in the direction of the star. The process is essentially identical to the one above, except with the stellar SED already known, the atmospheric transmission falls out without requiring a lidar to measure monochromatic transmissions. This metadata stream will be useful for other telescopes observing in that or nearly the same direction, reducing or minimizing valuable large telescope time required for calibration. The atmospheric data is also of interest to a different set of scientists studying the atmosphere.

6. Summary

UNM and NIST will soon be producing a new generation of calibrated standards stars referenced to NIST detector-based standards. Using the combination of calibrated spectrophotometry and calibrated elastic backscatter lidar, the primary impediment to accomplishing this task, measuring and removing the signature of atmospheric transmission, is surmountable.

Acknowledgments. This research is supported by NIST Award 60NANB9D9121 and NSF Grant AST-1009878.

References

Berk, A., Anderson, G. P., Acharya, P. K., Bernstein, L. S., Muratov, L., Lee, J., Fox, M., Adler-Golden, S. M., Chetwynd, J. H., Hoke, M. L., Lockwood, R. B., Gardner, J. A., Cooley, T. W., Borel, C. C., & Lewis, P. E. 2005, vol. 5806, 662. URL http://adsabs.harvard.edu/abs/2005SPIE.5806..662B

Bevis, M., Businger, S., Chiswell, S., Herring, T. A., Anthes, R. A., Rocken, C., & Ware, R. H. 1994, Journal of Applied Meteorology, 33, 379. URL http://journals.ametsoc.org/doi/abs/10.1175/1520-0450%281994%29033%3C0379%3AGMMZWD%3E2.0.CO%3B2

Bohlin, R. C. 2000, The Astronomical Journal, 120, 437. URL http://adsabs.harvard.edu/abs/2000AJ....120..437B

Bohlin, R. C., & Gilliland, R. L. 2004, The Astronomical Journal, 127, 3508. URL http://adsabs.harvard.edu/abs/2004AJ....127.3508B

Brown, S. W., Eppeldauer, G. P., & Lykke, K. R. 2006, Applied Optics, 45, 8218. URL http://adsabs.harvard.edu/abs/2006ApOpt..45.8218B

Engelke, C. W., Price, S. D., & Kraemer, K. E. 2010, The Astronomical Journal, 140, 1919. URL http://adsabs.harvard.edu/abs/2010AJ....140.1919E

Hayes, D. S., & Latham, D. W. 1975, The Astrophysical Journal, 197, 593. URL http://adsabs.harvard.edu/abs/1975ApJ...197..593H

Hayes, D. S., Latham, D. W., & Hayes, S. H. 1975, The Astrophysical Journal, 197, 587. URL http://adsabs.harvard.edu/abs/1975ApJ...197..587H

Heap, S. R., & Lindler, D. J. 2007, vol. 374, 409. URL http://adsabs.harvard.edu/abs/2007ASPC..374..409H

Kojima, J., & Nguyen, Q. 2002, Applied Optics, 41, 6360. URL http://ao.osa.org/abstract.cfm?URI=ao-41-30-6360

Kovalev, V. A., & Eichinger, W. E. 2004, Elastic lidar : theory, practice, and analysis methods (Hoboken, N.J.: Wiley)

Larason, T., Bruce, S., & Cromer, C. 1996, Journal of Research of the National Institute of Standards and Technology, 101, 133. URL http://nvlpubs.nist.gov/nistpubs/jres/101/2/j2lara.pdf

Megessier, C. 1995, Astronomy and Astrophysics, 296, 771. URL http://adsabs.harvard.edu/abs/1995A%26A...296..771M

Mountain, C. M., Selby, M. J., Leggett, S. K., Blackwell, D. E., & Petford, A. D. 1985, Astronomy and Astrophysics, 151, 399. URL http://adsabs.harvard.edu/abs/1985A%26A...151..399M

Oke, J. B., & Schild, R. E. 1970, vol. 2, 212. URL http://adsabs.harvard.edu/abs/1970BAAS....2Q.212O

Peterson, D. M., Hummel, C. A., Pauls, T. A., Armstrong, J. T., Benson, J. A., Gilbreath, G. C., Hindsley, R. B., Hutter, D. J., Johnston, K. J., Mozurkewich, D., & Schmitt, H. R. 2006, Nature, 440, 896. URL http://adsabs.harvard.edu/abs/2006Natur.440..896P

Smith, A. W., Woodward, J. T., Jenkins, C. A., Brown, S. W., & Lykke, K. R. 2009, Metrologia, 46, 219. URL http://adsabs.harvard.edu/abs/2009Metro..46S.219S

Tüg, H., White, N. M., & Lockwood, G. W. 1977, Astronomy and Astrophysics, 61, 679. URL http://adsabs.harvard.edu/abs/1977A%26A....61..679T

van Leeuwen, F., Evans, D. W., Grenon, M., Grossmann, V., Mignard, F., & Perryman, M. A. C. 1997, Astronomy and Astrophysics, 323, L61. URL http://adsabs.harvard.edu/abs/1997A%26A...323L..61V

Yoon, H. W., Butler, J. J., Larason, T. C., & Eppeldauer, G. P. 2003, Metrologia, 40, 154. URL http://adsabs.harvard.edu/abs/2003Metro..40S.154Y

Zimmer, P. C., McGraw, J. T., Ackermann, M. R., Hines, D. C., Hull, A. B., Rossmann, L., Zirzow, D. C., Brown, S. W., Cramer, C. E., Fraser, G. T., Lykke, K. R., Smith, A. W., Stubbs, C. W., & Woodward, J. T. 2010, vol. 7735, 272. URL http://adsabs.harvard.edu/abs/2010SPIE.7735E.272Z